ELSEVIER

Journal of Molecular Catalysis A: Chemical 181 (2002) 41–55

JOURNAL OF MOLECULAR CATALYSIS A: CHEMICAL

www.elsevier.com/locate/molcata

Effects of surface modification on coking, deactivation and *para*-selectivity of H-ZSM-5 zeolites during ethylbenzene disproportionation

Wen-Hua Chen [a], Tseng-Chang Tsai [b,1], Sung-Jeng Jong [a,2], Qi Zhao [a], Chung-Ta Tsai [a,c], Ikai Wang [d], Huang-Kuei Lee [c], Shang-Bin Liu [a,*]

[a] *Institute of Atomic and Molecular Sciences, Academia Sinica, P.O. Box 23-166, Taipei 106, Taiwan, ROC*
[b] *Department of Chemical Engineering, I-Shou University, Kachsiung 840, Taiwan, ROC*
[c] *Institute of Materials Science and Manufacturing, Chinese Culture University, Taipei 111, Taiwan, ROC*
[d] *Department of Chemical Engineering, National Tsinghua University, Hsinchu 300, Taiwan, ROC*

Received 24 January 2001; received in revised form 9 April 2001; accepted 22 June 2001

Abstract

The effects of coking and surface modification of H-ZSM-5 zeolites on enhancement of *para*-diethylbenzene selectivity during disproportionation of ethylbenzene have been investigated. Surface modifications of the zeolites by silica chemical vapor deposition (Si-CVD) and by stepwise lepidine adsorption and/or Si-CVD treatments were examined. The acidity, sorption capacity, stability, and coke content of the samples were characterized by various techniques, such as adsorption, TGA, IR, ^{129}Xe NMR, and solid-state ^{27}Al and ^{31}P MAS NMR. The performance of the *para*-selective process was studied by the correlation between the observed *para*-selectivity and conversion. The working principle responsible for the *para*-selective feature was found due to the combined effects of diffusion limitations and inactivation of external active sites. At the extreme of low conversion, the feature depends mostly on the former effect, whereas the latter becomes progressively important with increasing conversion. At high conversion, while both effects are important, diffusion controlled limitations associated with steric hindrances near the pore mouths plays the predominant role, especially towards saturating surface SiO_2 loading.

Keywords: Shape selectivity; Si-CVD; Coking; H-ZSM-5 zeolite; NMR

1. Introduction

Para-diethylbenzene (*p*-DEB) is a high-valued desorbent commonly used in *p*-xylene adsorptive separation processes [1] and the key starting material of vinylstyrene, whereas its isomers, *o*- and *m*-DEB, have lower market values. Although *p*-DEB can be produced by the ethylbenzene (EB) disproportionation, a model reaction widely used for the characterization of catalytic activity of zeolites [2–5], the yield is normally limited by the thermodynamic equilibrium

* Corresponding author. Tel.: +886-2-2366-8230; fax: +886-2-2362-0200.
E-mail addresses: tctsai@isu.edu.tw (T.-C. Tsai), sbliu@sinica.edu.tw (S.-B. Liu).
[1] Co-corresponding author. Tel.: +886-7-657-7711x3414; fax: +886-7-657-8945.
[2] Present address: Union Chemical Laboratory, Industrial Technology Research Institute, Hsinchu 300, Taiwan, ROC.

1381-1169/02/$ – see front matter
PII: S1381-1169(01)00355-7

compositions. The development and improvement of *para*-selective process not only simplify the production schemes but also significantly reduce the production costs. Thus, research on *para*-selectivity enhancement is an important and challenging task with great industrial demands.

Many *para*-selective processes have been developed for important industrial applications, for examples, alkylation, disproportionation and isomerization of monoalkylbenzene, using a variety of different catalyst modification techniques, such as surface deposition of SiO_2 [6–20] or oxides of P, B or Mg [8,20–29], or by pre-coking [30–33]. In spite of extensive research in this field, the nature of the related shape selective process is still not well understood and the subject of ongoing debates [8,14,19,33–38]. It was proposed that the *para*-selective feature is provoked by diffusion limitations due to pore narrowing/blocking and/or by inactivation of external acidity which inhibits the secondary, non-shape selective isomerization reactions on the surface of the catalyst.

The objectives of this study is to investigate how coking interplay with the types and extents of catalyst surface modification treatments and their respective roles during the decisive working principles of the *para*-selective process. In particular, the effects of coke deposition, surface modification by silylation and/or molecular adsorption, and reaction conditions on the activity and *p*-DEB selectivity of H-ZSM-5 zeolites during EB disproportionation were examined. The nature and acidity of the catalysts were characterized by diffuse reflectance Fourier-transform infrared spectroscopy (DRIFTS), solid-state ^{27}Al magic-angle-spinning (MAS) NMR and ^{31}P MAS NMR spectroscopy of the adsorbed phosphine oxide probe molecules. Whereas the variations of sorption capacity and the location/concentration of coke deposits in the catalysts were determined by xenon adsorption, ^{129}Xe NMR, and thermogravimetric analysis (TGA), respectively.

2. Experimental

2.1. Materials

The powdered, binderless parent H-ZSM-5 zeolite ($Si/Al = 15$; denoted as HZSM5) was obtained commercially (Stream Chemical), its structure and framework compositions were confirmed by powder X-ray diffraction (XRD) and ^{29}Si MAS NMR. The amount of NH_3 retained in the sample at 473 K was $0.79\,mmol\,g^{-1}$ catalyst. An average crystalline size of 0.5 μm for the zeolite sample was determined by electron microscopy. Research grade reagents were obtained commercially and were used without further purification.

2.2. Silica chemical vapor deposition (Si-CVD)

Surface modified, silylated samples were prepared by chemical vapor deposition of silica (Si-CVD), using TEOS as the silylation agent, following the procedures reported earlier by Wang et al. [8]. Pelletized parent HZSM5 zeolite (10–20 mesh; ca. 4 g) was first packed into a home-built reactor, followed by calcination at 723 K in air (flow rate 100 ml/min) for 8 h, then brought to 413 K under stream of N_2 gas (100 ml/min). Silylation treatment of samples were conducted by passing mixture of 4 wt.% TEOS in toluene through the catalyst bed at 413 K under N_2 carrier gas ($12\,ml\,h^{-1}$) for various deposition time (t_d), subsequently followed by calcination in flowing air (100 ml/min) at 823 K for 4 h. The effectiveness of the treatment was monitored by analyzing the residual TEOS in the reactor effluent at various t_d. Accordingly, samples with varied amount of deposited SiO_2 were obtained (Table 1). They are identified by Si/HZSM5 followed by the duration of deposition t_d, for example, Si/HZSM5-6 means the parent (HZSM5) zeolite was modified by one Si-CVD cycle for $t_d = 6$ h. A sample modified with two Si-CVD treatment cycles (denoted as Si/HZSM5-6/2) was prepared by a sample first silylated by one Si-CVD cycle with $t_d = 6$ h, calcined and subsequently followed by second Si-CVD treatment for additional 2 h (i.e. $t_d = 6 + 2$ h) and the calcination treatment.

2.3. Surface modification by stepwise surface adsorption and Si-CVD

In separate experiments, stepwise surface modification by lepidine adsorption (LA) and Si-CVD treatments were achieved using a different HZSM5 zeolite ($Si/Al = 40$; crystalline size ca. 0.8 μm; Zeolyst).

Table 1
The coke content and deactivation parameters during EB disproportionation over parent and SiO_2 modified Si/HZSM5 zeolites[a]

Samples	t_d[b] (h)	SiO_2 content (wt.%)	Coke content (wt.%)	Deactivation parameters[c]				σ_{Xe}[d]		V/V_0 (%)	
				X_0	k	α	$X_0 + k$[e]	Fresh	Coked	Fresh	Coked
HZSM5[f]	–	–	2.6	44.0	7.3	1.93	51.3	4.14	4.42	100	93.7
Si/HZSM5-2	2	11.5	3.3	34.7	7.7	0.19	42.4	4.22	4.90	98.1	84.6
Si/HZSM5-6	6	14.5	2.8	30.7	11.5	0.25	42.2	4.28	4.98	96.7	83.1
Si/HZSM5-6/2[g]	6 + 2[g]	18.2	4.0	21.6	8.6	0.54	30.2	4.40	5.01	94.1	82.6

[a] Reaction conditions: $T_r = 573$ K; WHSV $= 1.85\,h^{-1}$; pressure $= 1\,kg\,cm^{-2}$; carrier gas: N_2; N_2/EB $= 2.0$ mol/mol, TOS $= 9$ h.
[b] Deposition time of the Si-CVD treatment.
[c] Calculated from Eq. (1).
[d] In unit of (ppm/atom g^{-1}) $\times 10^{20}$.
[e] In unit of wt.%; represents the conversion at TOS $= 0$ h.
[f] Parent HZSM5 zeolite.
[g] Prepared by two deposition cycles; the sample prepared by $t_d = 6$ h during the first cycle was calcined at 773 K in air for 6 h followed by a second treatment for additional 2 h.

The results obtained from these experiments should provide supporting evidence that enable us to compare the effect of surface adsorption and silylation on the variations of external acidity and *para*-selective feature of the catalyst. The feasibility of such comparison is warranted by the fact that the size of lepidine molecule is much greater than the pore aperture of HZSM5 and thus can only be adsorbed on the external surface of the zeolite [39]. Different samples modified by LA (sample LA) and/or Si-CVD treatment (sample CVD) were prepared (Table 2). The sample denoted LA-CVD represents deposition of SiO_2 (at 413 K; 6 h) after saturate adsorption of lepidine, then followed by regular calcination treatment. Whereas the sample denoted LA-CVD-LA represents further adsorption of lepidine on a sample having the same preparation procedure with sample LA-CVD.

2.4. Ethylbenzene disproportionation reaction

Ethylbenzene disproportionation was used as test reaction [2–5] throughout this study. The reaction was conducted in a continuous flow, fixed-bed microreactor (stainless steel; 15 mm i.d.) under the standard conditions: reaction temperature (T_r) $= 573$ K, space velocity (WHSV) $= 1.85$–$6.60\,h^{-1}$, pressure $= 1\,kg\,cm^{-2}$, carrier gas-to-feed ratio (N_2/EB) $= 2.0$ mol/mol, and time-on-stream (TOS) $= 9$ h. The compositions of the reactor effluent were analyzed in situ by gas chromatography (Shimadzu GC-9A) using a packed column [40]. Upon completion of experiment, the fouled (coked) catalyst was first purged with N_2 gas at T_r for 0.5 h, then maintained at 473 K for at least 6 h before it was finally brought down to room temperature (298 K).

Table 2
Catalytic performances during EB disproportionation over parent and surface modified HZSM5 zeolite samples[a]

Catalysts	Parent	LA	LA-CVD	LA-CVD-LA	CVD
SiO_2 content (wt.%)	–	–	9.5	9.5	9.4
WHSV (h^{-1})	2.23	1.17	0.82	0.41	0.82
Conversion (wt.%)[b]	27.4	28.7	27.8	28.8	27.9
p-DEB/DEB (%)	30.4	34.1	38.9	47.2	56.6

[a] Si/Al $= 40$.
[b] Reaction conditions: $T_r = 573$ K, TOS $= 0.25$ h and maintained at a constant conversion of ca. 28 wt.% by careful adjustment of WHSV.

To compare the performance of samples prepared during the stepwise surface modification experiments, reactions were carried out for all samples at about the same conversion (ca. 28 wt.%; by careful adjustment of WHSV) under similar conditions: $T_r = 573$ K and TOS = 0.25 h (Table 2).

2.5. Characterization methods

Infrared spectroscopy (DRIFTS; Bruker IFS-28) was utilized to characterize acidity and the nature of coke deposits in the sample. Sample was dehydrated in situ at 473 K for at least 3 h before each run. The amount of coke deposits in the sample, measured by TGA (ULVAC TGD-7000RH), was determined from the weight loss observed in the thermogram between 573 and 973 K. Xenon adsorption isotherms were measured at room temperature. All ^{129}Xe NMR spectra were obtained by a NMR spectrometer (Bruker MSL-300P) operating at the Larmor frequency of 83.012 MHz, using diluted xenon gas as the chemical shift reference. Detailed description of the related experimental setups and procedures of the above experiments have been described earlier [40].

The variations of Al coordination in the structural framework of zeolites were determined by solid-state ^{27}Al MAS NMR [41]. Whereas the changes in catalyst acidity upon sample surface modification were characterized by ^{31}P MAS NMR of two different adsorbed probe molecules [42–45], namely, TMPO and TBPO. It is noted that, unlike TMPO whose molecular size is comparable to the pore aperture of the HZSM5 zeolite, TBPO molecule is too big to enter the intracrystalline channel [46]. All ^{27}Al and ^{31}P MAS NMR spectra were obtained by a separate spectrometer (Bruker MSL-500P) operating at 130.32 and 202.46 MHz, using $Al(H_2O)_6^{3+}$ and 85% H_3PO_4 solution as the chemical shift reference, respectively. Typical sample spinning rate was 5–12 kHz, depending on the NMR probehead used. Moreover, except for the ^{27}Al NMR experiments in which fully hydrated samples were examined, dehydrated (723 K under vacuum; more than 24 h) samples were used during the ^{31}P NMR experiments. For these experiments, a known amount of TMPO or TBPO (dissolved in dry CH_2Cl_2) was introduced into a vessel containing dehydrated sample, and the mixture was agitated overnight under N_2 over an ultrasonic shaker. After removal of solvent by evacuation, the sample vessel was then placed into a glovebox (under N_2 environment) in which sample was transferred into a ZrO_2 MAS NMR rotor (4 mm o.d.) and sealed by gastight Kel-F cap.

3. Results

3.1. Surface modification by Si-CVD treatment

It was found that the conversion of TEOS was nearly 100% during initial ($t_d < 1$ h) Si-CVD treatment of the sample, subsequently followed by a rapid decrease associated with the progressive decrease in the available deposition sites on the external surface of the zeolite (not shown). Eventually, a plateau at null conversion ('apparent' saturation) occurred at $t_d \sim 6$ h. The resultant surface SiO_2 contents for samples Si/HZSM5-2 and Si/HZSM5-6 were 11.5 and 14.5 wt.%, respectively (Table 1). When the sample was subjected to second Si-CVD treatment, a steeper decrease in TEOS conversion was found and the point at which 'apparent' saturation of TEOS also occurred at a much shorter t_d. The deficiency of available deposition sites after the first Si-CVD treatment cycle was evidenced by the marginal increase in deposited SiO_2 during the second CVD cycle (Table 1).

3.2. Coking and catalytic performance during EB disproportionation

The conversion and *p*-DEB selectivity versus TOS during EB disproportionation over the parent (HZSM5) and Si-CVD modified (Si/HZSM5) zeolites are depicted in Fig. 1. The correlation between EB conversion with TOS can be fitted by an exponential function

$$X_t = X_0 + k\mathrm{e}^{-\alpha t} \quad (1)$$

where X_t represents the conversion at a given time t, X_0 and k the constants, and the exponent α is the parameter accounts for deactivation rate. The results of the fitting are depicted in Table 1 and Fig. 1a. Both the initial conversion ($X_0 + k$) and the deactivation rate (α) are found to decrease upon sample silylation treatment, which is in line with the observed increase in coke content. However, upon increasing severity of

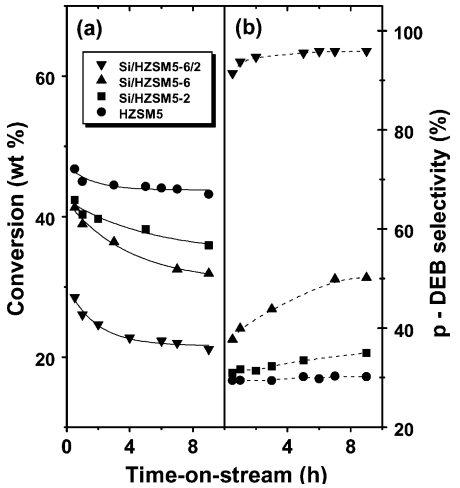

Fig. 1. The variations of (a) EB conversion; and (b) *p*-DEB selectivity with TOS during EB disproportionation over parent HZSM5 and Si/HZSM5 zeolites. Reaction conditions: $T_r = 573\,K$; WHSV $= 1.85\,h^{-1}$; pressure $= 1\,kg\,cm^{-2}$; carrier gas: N_2; N_2/EB $= 2.0$ mol/mol. The solid curves represent the results of fitting by Eq. (1).

surface silylation, a slight increase in deactivation rate was also observed, indicating a slight decrease in catalytic stability, especially for sample Si/HZSM5-6/2. The *p*-DEB selectivity increased with increasing SiO_2 content and a more drastic increase is evident for Si/HZSM5-6/2, which was subjected to additional silylation treatment, as shown in Fig. 1b and Table 3. However, comparing to the other modified samples, the leap selectivity increase for Si/HZSM5-6/2 is seemingly at the expense of conversion.

Prominent factors that could affect the activity and performance of zeolites include their structural and acid properties as well as the operation conditions applied during catalytic reaction. Here, the interplay of the related experimental parameters, such as severity of surface silylation, coke content, reaction conditions, and conversion level, during EB disproportionation over various samples is examined by the correlation of *p*-DEB selectivity with conversion, as shown in Fig. 2. In this context, data obtained at constant WHSV $= 1.85\,h^{-1}$ (during TOS = 0–9 h) are plotted along with those obtained at different WHSV (i.e. 3.17, 4.75 and $6.60\,h^{-1}$; obtained during TOS from 9 to 10.5 h). Interestingly, the observed *p*-DEB selectivity for each sample correlates well with the conversion in despite of the fact that the results were obtained from different WHSV and TOS (and thus different coke contents). Moreover, the results obtained from different samples all merge to a conversion of 46.8 wt.% corresponding to a selectivity value of 29.4%, which coincides with the thermodynamic equilibrium compositions: *m*-:*p*-:*o*-DEB = 69:28:3 revealed earlier by Mishin et al. [47].

For Si/HZSM5-6/2, the results can be fitting by a polynomial function to the fourth order, as illustrated

Table 3
Product distribution during EB disproportionation over parent and surface modified Si/HZSM5 zeolites[a]

Samples	HZSM5	Si/HZSM5-2	Si/HZSM5-6	Si/HZSM5-6/6
SiO_2 content (wt.%)	0[b]	11.5	14.5	18.2
Conversion[c] (wt.%)	42.8	35.9	31.9	21.1
Selectivity[c] (wt.%)				
p-DEB	15.6	18.6	24.8	54.7
m-DEB	34.4	36.7	24.6	2.4
o-DEB	1.6	0.3	0.0	0.0
Benzene	31.8	31.0	35.4	31.1
Toluene	3.5	3.1	3.8	3.0
Xylene	2.0	1.8	1.7	0.1
Others	11.2	8.4	9.6	8.8
p-DEB selectivity[c,d] (%)	30.2	33.5	50.2	95.9

[a] Reaction conditions: $T_r = 573\,K$; WHSV $= 1.85\,h^{-1}$; TOS = 0–9 h.
[b] Parent HZSM5 zeolite.
[c] Obtained at TOS = 9 h.
[d] Defined as: *p*-DEB selectivity = (amount *p*-DEB)/(total amount of DEB isomers).

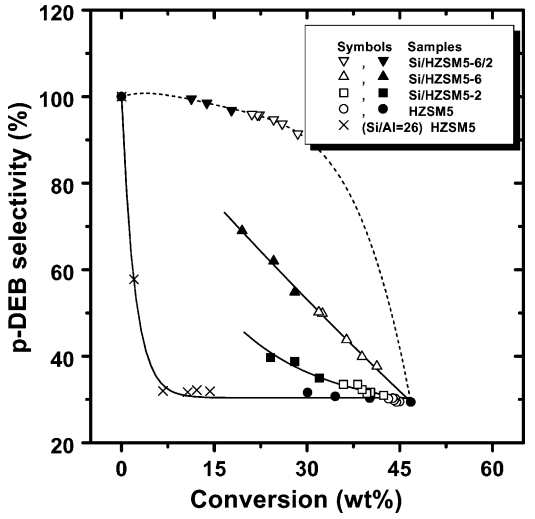

Fig. 2. The correlation of *p*-DEB selectivity with conversion for the coked Si/HZSM5 samples with various amounts of SiO_2 deposition. Data with open symbols were obtained from a fixed WHSV = 1.85 h^{-1} during TOS = 0–9 h, those with filled symbols were obtained with varied WHSV (3.17, 4.75 and 6.60 h^{-1}) during the TOS = 9–10.5 h. Data with (×) symbol were obtained from [39] (Si/Al = 26). The solid curves are the results of fitting by an exponential decay. The dashed curve represents the result of fitting by a polynomial function to the fourth order.

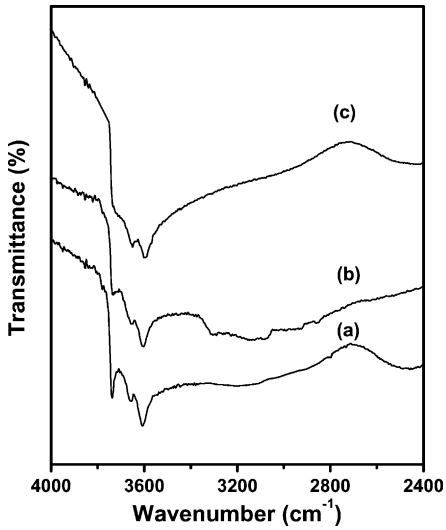

Fig. 3. IR spectra obtained from (a) parent HZSM5 zeolite, and surface modified sample prepared by (b) lepidine adsorption; and (c) silica deposition (sample Si/HZSM5-6/2).

in Fig. 2. Whereas for the parent HZSM5, *p*-DEB selectivity is nearly independent of conversion and maintains at 29.4% near to the thermodynamic equilibrium value [47], except at the extreme of low conversion. Previous results [40] obtained from a different HZSM5 sample (Si/Al = 26; crystalline size ca. 0.3 μm; Strem) operated under similar conditions (T_r = 573 K; N_2/EB = 2.0; WHSV = 7.4 h^{-1}) are also depicted in Fig. 2. Assuming that the selectivity is 100% at zero conversion, together with the observed value of 29.4% at 46.8 wt.% conversion, the results fit well to an exponential decay. The result of such fitting is shown in Fig. 2 together with that of Si/HZSM5-2 and Si/HZSM5-6; which also showed the similar dependence. Furthermore, at a given conversion, *p*-DEB selectivity tends to increase with increasing surface SiO_2 content.

3.3. Infrared spectroscopy study

The IR spectrum for the parent sample is shown in Fig. 3a. The absorption peak at 3610 cm^{-1} is assigned [48–51] due to the stretching vibration of the bridging hydroxyl groups affiliated with the tetrahedral-coordinated framework Al (Al^{F}_{tet}; i.e. Brønsted acid sites) which are predominately located within the intracrystalline channels of the zeolite. Whereas the absorption band at 3745 cm^{-1} can be attributed to the stretching vibration of the terminal SiOH (silanol) groups, which present mostly on the extracrystalline surface of the zeolite or at the defect sites. The weak band at ca. 3650 cm^{-1} is ascribed due to hydroxyl groups associated with the octahedral-coordinated non-framework Al (Al^{NF}_{oct}) species. Upon saturation adsorption of lepidine (Fig. 3b), the absorption band at 3745 cm^{-1} nearly diminished while only a slight decrease in the intensity of the 3610 cm^{-1} band was found compared to Fig. 3a. Sample surface modification by silylation also tends to affect both the silanol and Brønsted sites, as shown in Fig. 3c.

Fig. 4 displays the IR spectra of HZSM5 and Si/HZSM5 samples obtained before and after EB disproportionation. The spectra obtained from the fresh (unreacted) samples (Fig. 4a) clearly show a marked decrease of the bands corresponding to silanol and Brønsted acid sites upon first silylation treatment of the parent sample.

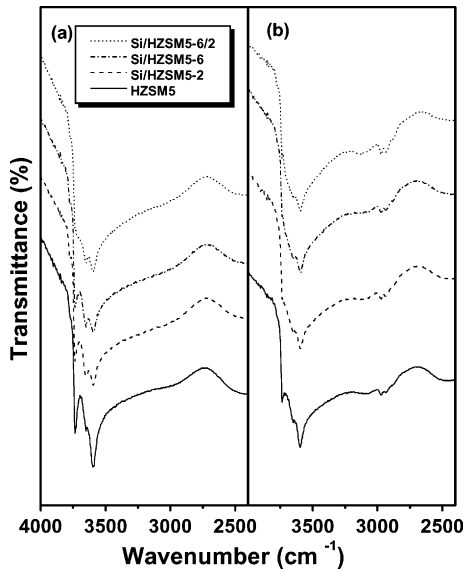

Fig. 4. IR spectra of the parent HZSM5 and silica deposited Si/HZSM5 samples obtained (a) before; and (b) after the EB disproportionation reaction.

A slight increase in intensity of the 3650 cm^{-1} band arising from the Al^{NF}_{oct}–OH species was also found. Increasing severity of surface silylation resulted in a progressive decrease of the SiOH band at 3745 cm^{-1} and a slight increase of the Al^{NF}_{oct}–OH band at 3650 cm^{-1}, while the band at 3610 cm^{-1} (SiOHAl) remains practically unchanged. Moreover, the SiOH band nearly vanished for Si/HZSM5-6/2 with an optimal surface SiO_2 content of 18.2 wt.%.

The IR spectra for fouled (coked) samples are shown in Fig. 4b. Additional weak absorption bands in the 2800–3200 cm^{-1} region were found. These bands are ascribed to the C–H vibrational modes of the carbonaceous compounds [48,49]. More specifically, the absorption bands in the range 2800–3000 cm^{-1} can be ascribed to the presence of aliphatic (soft) coke, whereas the weaker bands in the range 3000–3200 cm^{-1} correspond to bulkier aromatic or polyaromatic (hard) coke [40,52]. Moreover, marked decrease in the SiOH and Al^{NF}_{oct}–OH band intensities were observed compare to the fresh samples in Fig. 4a, whereas the intensity of the SiOHAl band remained practically unchanged.

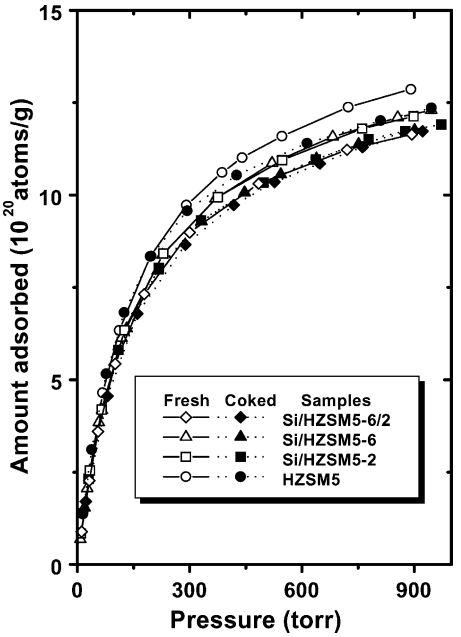

Fig. 5. Xenon adsorption isotherms of the parent HZSM5 and silica deposited Si/HZSM5 samples obtained before (open symbols) and after (filled symbols) the EB disproportionation reaction.

3.4. Room temperature xenon adsorption and ^{129}Xe NMR studies

Room temperature xenon adsorption isotherms for various samples obtained before and after the reaction are shown in Fig. 5. For the fresh samples, a progressive decrease in adsorption capacity with increasing extent of silylation is evident. The same but much smaller effect was observed for the coked samples. The variations of ^{129}Xe NMR chemical shift with respective to xenon uptake for various samples are presented in Fig. 6. In this case, a progressive increase in ^{129}Xe chemical shift with increasing surface SiO_2 content was found for the fresh samples and a much weaker effect was observed for the coked samples. The concave chemical shift curves at low Xe loading are ascribed due to the presence of strong adsorption sites arising from solid-state defects or extra-framework Al in the zeolite channels [52].

The variations in the effective free volume of the fresh and coked samples can be correlated with the slope of the chemical shift curve (σ_{Xe}) at high Xe loading, which in principle reflects binary collisions

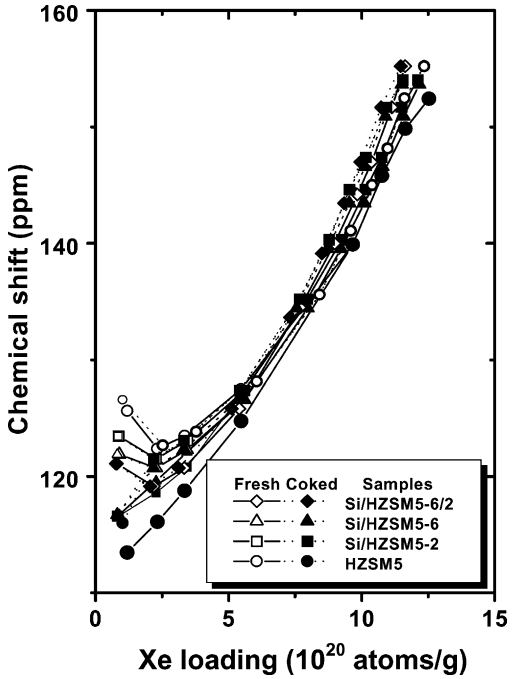

Fig. 6. The variations of ^{129}Xe NMR chemical shifts with xenon loading for the parent HZSM5 and silica deposited Si/HZSM5 samples obtained before (open symbols) and after (filled symbols) the EB disproportionation reaction.

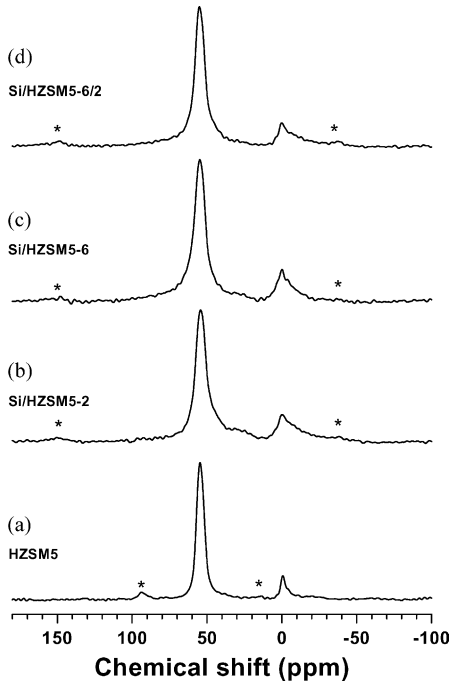

Fig. 7. The ^{27}Al MAS NMR spectra obtained from (a) parent HZSM5; (b) Si/HZSM5-2; (c) Si/HZSM5-6; and (d) Si/HZSM5-6/2 samples. The spectra were recorded with spinning rate of 12 or 5 kHz. The asterisks in the spectrum represent spinning sidebands.

of Xe [53]. Accordingly, the relative volume change for the fresh and coked samples can be, respectively, expressed as [40,52,54]

$$\left(\frac{V}{V_0}\right)_{\text{fresh}} = \frac{(\sigma_{\text{Xe}})_{\text{parent}}}{(\sigma_{\text{Xe}})_{\text{fresh}}} \quad (2)$$

$$\left(\frac{V}{V_0}\right)_{\text{coked}} = \frac{(\sigma_{\text{Xe}})_{\text{fresh}}}{(\sigma_{\text{Xe}})_{\text{coked}}} \quad (3)$$

where V_0 and V represent the internal free volume of the fresh (or coked) parent and Si/HZSM5 samples, respectively. The fractional volume change, V/V_0, in various samples before and after the reactions can thus be calculated based on Eqs. (2) and (3), as listed in Table 1. A slight decrease in relative free volume with increasing surface SiO_2 content was observed for both fresh and coked samples. Moreover, a more subtle decrease was clearly observed for samples after the silylation treatment, both before and after reaction. Overall, the results obtained from ^{129}Xe NMR are in accordance with that from xenon adsorption.

3.5. Solid-state ^{27}Al and ^{31}P MAS NMR studies

Solid-state ^{27}Al MAS NMR confirmed the existence of small amount (<7%) of extra-framework Al in the parent HZSM5 sample (Fig. 7a). The ^{27}Al resonance at chemical shifts 56 and 0 ppm can be assigned due to Al^{F}_{tet} and Al^{NF}_{oct} species, respectively. Upon surface silylation treatment, the amount of Al^{NF}_{oct} slightly increased but did not vary significantly with the amount of deposited SiO_2 (Fig. 7b–d).

^{31}P MAS NMR was utilized to investigate the effect of silica surface deposition on variations of internal and/or external acidity. Accordingly, the types and relative distribution of acid sites in the sample were monitored by the changes in ^{31}P chemical shifts arising from the phosphorus-based probe molecules,

TMPO or TBPO, adsorbed at different environments. The size of TMPO molecule, being comparable to the pore aperture of the HZSM5, is accessible to both internal and external acid sites of the zeolite. Whereas TBPO molecule is too big to enter the channels and hence can only be adsorbed on the external surface of the zeolite. Thus, more TMPO (1.0 mmol g^{-1} catalyst) were loaded onto the sample as compared to the case of TBPO (0.02 mmol g^{-1} catalyst). Consequently, more signal accumulation was required for sample loaded with TBPO (typically 8000–12,000 scans) than TMPO (800 scans) in order to obtained ^{31}P spectrum with adequate signal sensitivity.

All ^{31}P MAS NMR spectra of TMPO adsorbed on the parent HZSM5 and Si/HZSM5 samples revealed multiple overlapped peaks, as shown in Fig. 8a. The strong sharp peak at 30 ppm and the weaker broad peak at 43 ppm can both be assigned to physisorbed TMPO [42–45]. The presence of these resonance peaks confirms that the samples may have pasted the titration point of the acid sites, which readily form complexes with the TMPO. Presumably, these TMPO are weakly bound and may undergo rapid exchange thus resulted in narrower resonance line. On the other hand, the peaks at 53, 65 and 75 ppm can be attributed to TMPO associated with Brønsted acid sites [44,45]. It has been proposed that the formation of TMPO/Brønsted acid complexes be invoked by bonding of $TMPOH^+$ with the bridging oxygen [44]. The ^{31}P chemical shifts arising from this protonated TMPO species tend to move toward downfield as the degree of proton transfer increases. Thus, resonance peaks with higher chemical shifts are most likely due to stronger protonic acid species that has shorter H–O bonds.

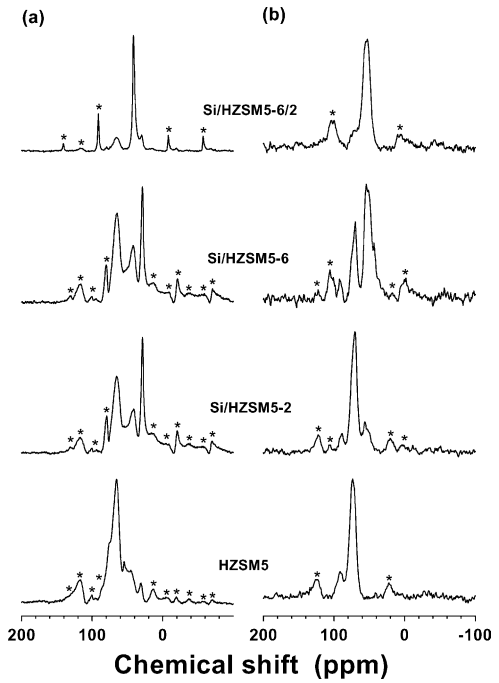

Fig. 8. The ^{31}P MAS NMR spectra of (a) 1.0 mmol of TMPO; and (b) 0.02 mmol of TBPO adsorbed per gram of parent HZSM5 or different surface modified Si/HZSM5 zeolites (see text). All spectra were recorded with a spinning rate of 10 kHz and were subjected to artificial line-broadening of 100 Hz. The asterisks in the spectrum represent spinning sidebands.

Upon sample modification by Si-CVD, notable simultaneous decrease in the overall Brønsted acidity and corresponding increase in the physisorbed TMPO peaks were observed. Comparing the ^{31}P spectra of the parent HZSM5 and Si/HZSM5-2 samples can readily see this. Moreover, the small shoulder peak at 75 ppm presented in HZSM5 also appeared to vanish upon sample silylation. Increasing deposition of surface SiO_2, for example, from 11.5 (Si/HZSM5-2) to 14.5 wt.% (Si/HZSM5-6), has relatively little effect on the observed ^{31}P spectrum. However, when the sample is subjected to an additional Si-CVD treatment cycle, as for Si/HZSM5-6/2, only a strong sharp peak at 43 ppm and two smaller peaks at 30 and 63 ppm appeared indicating that most of the TMPO were located on the external surface.

The ^{31}P MAS NMR spectra obtained from the parent and modified samples loaded with TBPO are shown in Fig. 8b. Similar work was not found in the existing literatures by the authors. Overall, five resonance peaks at 45, 55, 71, 75 and 92 ppm can be identified; the peak at 75 ppm appears as the shoulder of the peak at 71 ppm. By analogy of the assignments for TMPO above, we assign both peaks at 45 and 55 ppm as the physisorbed TBPO on the external surface of the sample. Whereas the further downfield resonance at 71, 75 and 92 ppm are attributed to the TBPO/Brønsted acid complexes on the external surface. In this context, the amounts of external acid site decrease upon increasing surface SiO_2 content, this was accompanied by simultaneous increase in physisorbed TBPO.

3.6. Stepwise surface modification by lepidine adsorption and silylation

By comparing results obtained from various samples listed in Table 2, a progressive increase in *p*-DEB selectivity with progressing stepwise treatments of the samples is observed. However, in view of *p*-DEB selectivity enhancement, surface modification by LA was not as efficient compare to the sample treated by silica deposition (CVD), which yielded a respective value of 34.1 and 56.6%. Surface modifications thus have definite effect on *p*-DEB selectivity enhancement for HZSM5 zeolite during EB disproportionation.

4. Discussion

4.1. Effects of surface modification and coking on acidity, activity, and structural and catalytic stability of the zeolite catalyst

Wang et al. [8] reported that the Si-CVD surface treatment is an acid catalysis reaction during which the rate of deposition depends strongly on the acidity of zeolites. More recently, Weber et al. [13] showed that Si-CVD method is superior to coating the catalyst with a silica shell, because external acidity can be eliminated without significantly changing the internal acidity of the catalyst [19]. Moreover, it has been proposed that, porosity of the zeolite and the reaction parameters (such as temperature and duration of deposition) used during silylation treatment all play important roles in the reaction site by which tailoring of the pore mouth opening can be achieved [13,17–20,55].

Our results show that, upon first silylation treatment of the parent sample, both the silanol and Brønsted acid sites are diminished, meanwhile, the amount of Al_{oct}^{NF} slightly increases. This can readily be seen by comparing the IR spectra (Fig. 4a) and ^{31}P NMR (Fig. 8a) of the fresh HZSM5 and Si/HZSM5-2 samples. Since the external acid sites is estimated less than 2% of the total acidity, the decrease in the overall acidity upon silylation is thus likely due to inactivation of external acid sites upon Si-CVD treatment associated with dealumination. The IR spectrum obtained directly from sample prepared after LA without the calcination treatment (Fig. 3b) provides supporting evidence to this argument, in which only the external active sites were affected. Presumably, dealumination could occur due to existence of trace amount of H_2O during hydrolysis reaction and/or subsequent calcination of the samples, as revealed by Fig. 4a. However, analysis of the ^{27}Al MAS spectra (Fig. 7) revealed no apparent trend in terms of relative concentration of Al_{tet}^{F} versus Al_{oct}^{NF}, regardless of the pre-existing Al_{oct}^{NF} species in the parent sample. Possible errors might arose from the presence of 'NMR-invisible' Al_{oct}^{NF} species which experienced large quadrupolar interactions under asymmetric environments [18,57–59]. The fact that Si/HZSM5 samples exhibit better catalytic stability than parent HZSM5, as revealed by the observed deactivation rates in Table 1, indicates that dealumination is most likely to occur at the internal Brønsted acid sites.

Moreover, that the ^{31}P resonance at 75 ppm (Fig. 8a) vanishes upon immediate sample silylation indicate that TEOS prefer to hydrolyzed at the strongest external Brønsted acidic sites. Presumably, these sites should locate near the pore mouths of the zeolite at which additional electrostatic interactions may be associated with structural irregularities or defects. Together with the fact that ^{31}P spectra are nearly invariant with SiO_2 contents (cf. two center spectra in Fig. 8a) render the effective inactivation of strong external acid sites upon sample Si-CVD treatment. The silanol sites, which are more abundant on the external surface and can be reached without steric constraints, are inactivated only when strong external acid sites accessible by TEOS during hydrolysis are preoccupied. As sample was subjected to second Si-CVD treatment, the competitively physisorbed species can be removed by evacuation or calcination, hence portions of the surface active sites can be re-exposed. It was implied by many authors that cyclic silylation is favorable in achieving complete inactivation of external surface acidity and a more uniform silica coverage [14–16,56]. However, based on the ^{31}P NMR spectrum obtained from TMPO adsorbed on Si/HZSM5-6/2 (Fig. 8a), it is clear that substantial steric hindrances was imposed on TMPO by the deposited SiO_2, thus prevent the probe molecules from entering the internal channels. In this context, deposition of SiO_2 near the pore mouths of the zeolite provoked by repeating CVD treatments can be inferred. Furthermore, that the 'strong' external acid sites responsible for ^{31}P resonance at higher chemical shifts on the spectrum obtained from either TMPO or TBPO

adsorbed on Si/HZSM5-6/2 (Fig. 8a and b) nearly vanished also indicates the effective removal of external acidity imposed by the second Si-CVD treatment.

In terms of adsorption capacity, the results obtained from Xe isotherms of the fresh and coked samples (Fig. 5) all show notable decrease upon sample silyation. Similar conclusion can be drawn from the ^{129}Xe NMR (Fig. 6) results, except in this case, ^{129}Xe chemical shifts show the expected opposite trend. This can be ascribed mainly due to the fragments of Al_{oct}^{NF} species retained in the channels of the modified zeolites and can readily be realized by the variations of $(V/V_0)_{fresh}$ or $(V/V_0)_{coked}$ (Table 1). That the variations of V/V_0 between parent HZSM5 and Si/HZSM5 is more pronounced than among Si/HZSM5 samples themselves confirms that dealumination occurs upon immediate Si-CVD treatment and preferentially takes place at the strong internal Brønsted acid sites. While repeating sample Si-CVD treatment also provokes further dealumination, the effect is somewhat weaker. Thus, in this context, the slight dealumination which occurs during sample silylation should not play significant role in the overall performance of the catalyst, particularly in the interplay of surface modification and coking on product shape selectivity to be discussed below.

On the other hand, the difference between $(V/V_0)_{fresh}$ and $(V/V_0)_{coked}$, respectively, obtained from the same sample before and after reaction, are attributed to the presence of coke deposits in the fouled samples. Furthermore, the slight decrease in the intensities of IR bands at 3745 and 3650 cm^{-1} for the coked (Fig. 4b) versus fresh (Fig. 4a) samples indicating that substantial amount of coke are preferentially located at the defect sites [52]. These coke deposits are mostly aliphatic in nature, as revealed in Fig. 4b. That the variations of V/V_0 for the fresh and coked (parent) HZSM5 is more pronounced comparing to the (modified) Si/HZSM5 is in line with the earlier notion that sample modification by Si-CVD provokes enhancement of catalytic stability of the zeolite catalyst.

4.2. Effects of surface modification and coking on shape selectivity

Prominent factors that could affect the product shape selectivity of the zeolite catalyst include microporosity, crystalline size [8,60], and diffusion barrier [34] which may arise from the presence of extra-framework Al [60,61] or intracrystalline coke [32]. Here, we focus on the investigation of the *para*-selective features of the HZSM5 zeolite, more specifically, by understanding the interplay of catalyst deactivation by coking and inactivation of external acidity by surface modification, using EB disproportionation as test reaction [2–5].

As shown in Fig. 2, high *para*-selectivity can be achieved at low conversion (say, <3 wt.%) even in the absence of surface SiO_2 deposition. However, at higher conversion (say, >6 wt.%), *p*-DEB selectivity maintains at the same level (29.4%) nearly coincide with the thermal equilibrium value in despite of the slight difference in the nature of zeolites [19]. Similar correlation has been reported for catalytic performance of alkylbenzene for other zeolites [19,32,34,47]. Furthermore, from the results obtained from different WHSV and TOS, the effect of coking on the *para*-selective properties of the sample can be inferred. For a given WHSV, conversion should decrease with increasing TOS and hence increasing coke deposits in the sample. The effect, which is more pronounced during the initial stage of the reaction [52], can be realized by following the open symbols in Fig. 2 (from right to left). Presumably, increase in acidity (or lower Si/Al) of zeolite would cause an increase in conversion thus more unfavorable for *para*-selectivity enhancement. Upon increasing WHSV, a higher *para*-selectivity but lower conversion and deactivation rate can be expected (cf. Fig. 2, filled symbols, right to left). Furthermore, at a given conversion, an increase in *p*-DEB selectivity with increasing surface SiO_2 content was observed (Fig. 2). In this case, a finite amount of coke deposits in the sample is expected. We note that, the typical coke content for the samples in the present study is less than 4 wt.% (Table 1). Thus, in this context, the observed increase in *p*-DEB selectivity with increasing surface SiO_2 content at constant conversion is mainly due to the inactivation of external active sites, while coking of the zeolite plays a minor role. Presumably, if the presence of coke deposits play a significant role, the observed *p*-DEB selectivity should deviate from the observed conversion dependent curve as TOS increases (cf. Fig. 2, from right to left). Inactivation of the surface acid sites by silylation treatment of HZSM5 zeolite thus has pronounced effect on *para*-selectivity

enhancement during EB disproportionation. Taking the conversion level of 30 wt.%, a value which is probably tolerable for practical applications, the *p*-DEB selectivity of ca. 31, 38, 52 and 90% can be anticipated for samples with surface SiO_2 content of 0, 11.5, 14.5 and 18.2 wt.%, respectively. Note that a leap increase in *p*-DEB selectivity was observed for Si/HZSM5-6/2 compare to the other Si/HZSM5 samples (vide infra).

Now, let us discuss the results of stepwise surface modification whose purpose was to investigate the effect of alternate removal/exposure of external surface active sites on *p*-DEB selectivity. As mentioned earlier, lepidine molecules, which exclusively adsorbed on the silanol sites and the Brønsted acid sites on the external surface, have a definite effect on *p*-DEB selectivity enhancement. However, the marginal increase in *p*-DEB selectivity for sample LA compare to the parent zeolite also revealing insufficient inactivation of external active sites, which may allow for non-selective isomerization reactions to occur on the external surface. As for sample LA-CVD, which was subjected to calcination during the Si-CVD treatment, lepidine molecules were removed and thus portions of the external active sites were re-exposed. Similar argument can be made for sample LA-CVD-LA. Note that for these samples subjected to silylation during the stepwise modification procedure, the amount of total surface SiO_2 was maintained at ca. 9.5 wt.%, for obvious purpose. Nevertheless, the observed *p*-DEB selectivity of 56.6% for sample CVD implies that this preset amount (9.5 wt.%) of SiO_2 is clearly not adequate to inactivate all of the external active sites. It is noted that a complete coverage of the external active sites is difficult to achieve by silylation treatment, mainly due to possible steric hindrance that may exist in the system. Weber et al. [15] recently reported an active sites coverage of 97% for HZSM5 zeolites by cyclic Si-CVD treatment.

Among the samples examined in this study, Si/HZSM5-6/2 appears to exhibit the best performance in terms of *p*-DEB selectivity enhancement. This particular sample, which was prepared by two Si-CVD modification cycles, exhibiting 96% *p*-DEB selectivity at a modest conversion level of ca. 20 wt.%. However, as evidenced by the ^{31}P NMR of the TMPO adsorbed on the sample, a large portion of the deposited silica might be located near the pore mouths and hence create enough steric constrains that prohibit the TMPO molecules to enter the intracrystalline channels of the zeolite. As a result, the formation of *o*- and *m*-DEB isomers are prohibited by product shape selectivity during EB disproportionation and thus resulted in the high *p*-DEB selectivity. Cyclic deposition by Si-CVD was found to provoke less selective deposition of silica which, in turn, resulted in pore mouth narrowing [16]. Niwa et al. [62] reported that covering of the external acidity of ZSM-5 could be achieved with the equivalent of six monolayers by Si-CVD method using TEOS as silylation agent. The threshold amount of deposited SiO_2 required for a substantial *para*-selectivity enhancement during alkylbenzene disproportionation was proposed to be ca. 10–13 wt.% [6,8,16,18]. However, the optimal amount of surface SiO_2 deposition should depend strongly on the operating conditions (e.g. temperature and duration of deposition) and silylation agent [13–16,19] applied as well as the crystalline size and acidity (concentration and strength of acid sites) of the zeolite [8] used. In this context, we thus attribute the high *p*-DEB selectivity observed for Si/HZSM5-6/2 sample due to not only the inactivation of external active sites but also diffusion limitations effect.

4.3. Para-selectivity of surface modified H-ZSM-5 zeolites during alkylbenzene disproportionation

As mentioned earlier, the genuine mechanism for the *para*-selectivity process during disproportionation/alkylation of alkylbenzene is still a controversial issue [14,19,33–38,63], among which, two mechanisms that involve the transport rate and product distribution of the dialkylbenzene isomers prevail, namely:

1. selective isomerization effect, which involves isomerization of the isomers within the zeolite channels, that is diffusion controlled by limitations due to steric hindrance near the channel opening or pore narrowing/blocking; and
2. non-selective isomerization effect, which involves further isomerization of the major product isomers on the external surface of the zeolite, that may be suppressed by inactivation of surface acidity.

However, it is often difficult to differentiate the two mechanisms one from the other. Because the parameters involved with the surface-related properties (e.g. surface area, crystalline size, conditions and extent of modification, etc.) are usually cross-linked to the kinetic or diffusion-related properties (e.g. diffusion rate, pore size, conversion, and relative concentration/size of the isomers, etc.). Thus, in terms of conversion and selectivity, the overall performance of the *para*-selective process is best discussed by roughly dividing the conversion into only the two extreme (low and high) regimes.

In this work, we observed that high *p*-DEB selectivity during EB disproportionation could be achieved for the unmodified HZSM5 zeolites only at very low conversion (<3 wt.%). Recently, Arsenova-Härtel et al. [38] examined the same system at low conversion (<2%) by oxalic acid treatments of samples with crystalline size of 0.02–0.05 and 2 μm. It was found that, while *m*- and *p*-DEB are reversibly sorbed into the HZSM5, *o*-DEB cannot enter the pore system in the temperature range 359–522 K. Moreover, the authors concluded that, isomerization of DEB proceeds exclusively inside the pores of zeolite. Thus, the *para*-selective features of the catalyst can be interpreted in terms of the interplay between catalytic reaction and mass transfer; surface inactivation has practically no effect on *para*-selectivity enhancement.

Our results obtained from the unmodified HZSM5 zeolites also indicate that, the reaction selectivity is kinetically controlled at low conversion, by which *para*-isomer is also known to be the primary product [9,14,36,64]. That all correlation curves in Fig. 2 can be fitted to 100% *p*-DEB selectivity at zero conversion provides an immediate support to this argument. Thus, in the extreme of low conversion, surface modification of the catalyst is probably redundant, because it should have negligible effect on *para*-selectivity enhancement. As the system moves toward slightly higher conversion (say, >3%), isomerization is likely to take place both in the internal channels and on the external surface of the zeolite. This is due to the fact that, isomerization occurs at a rate faster than disproportionation reaction by at least three orders of magnitude [65]. Since isomerization is a secondary process in this context, it will provoke the inter-conversion of the dialkylbenzene isomers. Thus, as the predominant *para*-isomers emerge out toward the external surface of the zeolite, they will be catalyzed by the external active sites immediately. This effect will be more pronounced when zeolites with smaller crystalline size were used [34]. Accordingly, the overall *para*-selective performance would be deteriorated. In other words, upon slight increasing in conversion, the *para*-selective process leans more weights toward surface-related properties. Inactivation of external active sites by sample surface modification, which serves the purpose of inhibiting these secondary, non-selective isomerization reactions, is thus an inevitable working principle in sustaining the high performance of the *para*-selective process. However, one should bear in mind that such modification treatment will be cross-linked with the diffusion-related properties and hence the overall performance in *para*-selectivity enhancement should be considered as the combined effect of diffusion limitations and inactivation of external acidity. In this context, the overall performance of *p*-DEB selectivity observed for sample Si/HZSM5-2 (Fig. 2) and those listed in Table 2 for the stepwise surface modification studies should fit themselves to this category.

At the other extreme, say, a high conversion of ca. 20–30% (typical for industrial operation), the isomerization reaction take place within the zeolite channels should always fulfill the conditions governed by kinetic principle and thus leading to the formation of thermodynamic equilibrium DEB isomer mixtures. Obviously, at this point, diffusion limitation should begin to play the key role in terms of the overall performance of the *para*-selective process. Because the diffusion rates of DEB isomers follow the trend: *p*-DEB $\gg$ *m*-DEB $>$ *o*-DEB, hence *p*-DEB should diffuse out of the pore more rapidly. Again, they will be immediately catalyzed by the secondary isomerization as they emerge out toward the external surface of the zeolite and hence resulted in a decrease in the overall *para*-selectivity. Thus, the inactivation of external active sites by surface modification should play an important role in sustaining the high performance of the *para*-selective process at high conversion, as illustrated for sample Si/HZSM5-6 in Fig. 2.

As in the case of sample Si/HZSM5-6/2, which was obtained by two Si-CVD modification treatments, the observed high *p*-DEB selectivity is undoubtedly due to the association between diffusion effects and inactivation of surface active sites. The leap increase in

p-DEB selectivity observed for Si/HZSM5-6/2 compare to the other Si/HZSM5 samples (see Fig. 2) indicating that the product isomers seem to encounter a diffusion barrier, which associated with the marked increase in the relative ratio of *p*- to *m*-DEB diffusivity. Thus, in this context, the working principle for the *para*-selectivity is predominantly due to diffusion limitations, while inactivation of external active sites also contribute to the *para*-selectivity, it plays a secondary role.

5. Conclusions

The effects of coking and surface modification of HZSM5 zeolites on the performance of *para*-selective process during disproportionation of EB have been investigated by the correlation between conversion and *p*-DEB selectivity. While a slight increase in extra-framework Al (Al_{oct}^{NF}) was found during Si-CVD treatment, they have negligible effect during the *para*-selective process. Precluding such dealumination effect, surface silylation treatment effectively inactivate the external active sites without changing the internal acidity or the adsorption capacity and effective free volume of the zeolites.

The *p*-DEB selective process for the unmodified HZSM5 samples is strictly kinetic control at low conversion. For Si-CVD modified samples, EB conversion was found to decrease with increasing coke content, which also favor the *p*-DEB selectivity enhancement regardless of the surface SiO_2 content. At a given conversion, notable increase in *p*-DEB selectivity with increasing SiO_2 content was observed. Coke deposits, which are found to locate mostly in the intracrystalline defect sites of the zeolite, play only a minor role during the *para*-selective process compare to inactivation of external active sites by silylation. Similar conclusion can be made for sample modified by surface adsorption of lepidine. Moreover, cyclic Si-CVD treatment of the zeolite sample was found to provoke non-selective deposition of silica on the external surface that create additional steric constraints for the DEB isomers to diffuse out of the channels, consequently, a leap increase in *p*-DEB selectivity was observed. Thus, inactivation of external active sites and diffusion limitations both play the decisive role in the enhancement of *para*-selectivity during disproportionation over HZSM5. Substantial inactivation of surface active sites is inevitable in provoking substantial relative increase in *p*- versus *m*-DEB diffusivity and thus, in turn, promoting the desirable *para*-selectivity enhancement.

Acknowledgements

The authors thank Prof. Kuei-Jung Chao, Dr. Ajit Pradhan and Dr. Jin-Fu Wu for helpful discussions. The financial supports of this work by the National Science Council, Taiwan, ROC (NSC87-2113-M001-003 and NSC88-2113-M001-008) are also gratefully acknowledged.

References

[1] J.D. Swift, M.D. Moser, in: Proceedings of the 20th Annual Meeting, 1995, DeWitt Petrochem. Rev.
[2] H.G. Karge, J. Ladebeck, Z. Sarbak, K. Hatada, Zeolites 2 (1982) 94.
[3] H.G. Karge, K. Hatada, Y. Zhang, R. Fiederow, Zeolites 3 (1983) 13.
[4] H.G. Karge, S. Ernst, M. Weihe, U. Weiss, J. Weitkamp, Stud. Surf. Sci. Catal. 84 (1994) 1805.
[5] Report of the IZA Catalysis Commission: IZA Newsletter No. 4, Zeolites 14 (1994) 387.
[6] M. Niwa, S. Kato, T. Hattori, Y. Murakami, J. Chem. Soc., Faraday Trans. I 80 (1984) 3135.
[7] J.P. Gilson, E.G. Derouane, J. Catal. 88 (1984) 538.
[8] I. Wang, C.L. Ay, B.J. Lee, M.H. Chen, in: Proceedings of the 9th International Congress on Catalysts, Calgary, Canada, 1988, p. 324.
[9] I. Wang, C.L. Ay, B.J. Lee, M.H. Chen, Appl. Catal. 54 (1989) 257.
[10] C.D. Chang, P.G. Rodewald, US Patent 5,498,814 (1996).
[11] J. Čejka, N. Žilková, B. Wichterlová, G. Eder-Mirth, J.A. Lecher, Zeolites 17 (1996) 265.
[12] Y.S. Bhat, J. Das, K.V. Rao, A.B. Halgeri, J. Catal. 159 (1996) 368.
[13] R.B. Weber, J.C.Q. Fletcher, K.P. Möller, C.T. O'Connor, Microp. Mesop. Mater. 7 (1996) 15.
[14] H.P. Röger, M. Krämer, K.P. Möller, C.T. O'Connor, Microp. Mesop. Mater. 21 (1998) 607.
[15] R.B. Weber, K.P. Möller, M. Unger, C.T. O'Connor, Microp. Mesop. Mater. 23 (1998) 179.
[16] R.W. Weber, K.P. Möller, C.T. O'Connor, Microp. Mesop. Mater. 35/36 (2000) 533.
[17] E. Klemm, M. Seitz, H. Scheidat, G. Emig, J. Catal. 173 (1998) 177.
[18] R.A. Shaikh, S.G. Kegde, A.A. Behlekar, B.S. Rao, Catal. Today 49 (1999) 201.
[19] T. Kunieda, J.H. Kim, M. Niwa, J. Catal. 188 (1999) 431.

[20] J. Das, A.B. Halgeri, Appl. Catal. A 194 (2000) 359.
[21] W.W. Kaeding, C. Chu, L.B. Young, B. Weinstein, S.A. Butter, J. Catal. 67 (1981) 159.
[22] W.W. Kaeding, C. Chu, L.B. Young, S.A. Butter, J. Catal. 69 (1981) 392.
[23] W.W. Kaeding, J. Catal. 95 (1985) 512.
[24] K.H. Chandawar, S.B. Kulkarni, P. Ratnasamy, Appl. Catal. 4 (1982) 287.
[25] J.H. Kim, S. Namba, T. Yashima, Stud. Surf. Sci. Catal. 46 (1989) 71.
[26] Z. Hu, W. Lihui, S. Chen, J. Dong, S. Peng, Microp. Mesop. Mater. 21 (1998) 7.
[27] Z. Hu, L. Wei, J. Dong, Y. Wang, S. Chen, S. Peng, Microp. Mesop. Mater. 28 (1999) 49.
[28] F. Lonyi, J. Engelhardt, D. Kallo, Zeolites 11 (1991) 169.
[29] Y.G. Li, H. Jun, Appl. Catal. A 142 (1996) 123.
[30] W.O. Haag, US Patent 4,097,543 (1978).
[31] G. Paparatto, E. Moretti, G. Leofanti, F. Gatti, J. Catal. 105 (1987) 227.
[32] J.L. Sotelo, M.A. Uguina, J.L. Valverde, D.P. Serrano, Appl. Catal. A 114 (1994) 273.
[33] L.Y. Fang, S.B. Liu, I. Wang, J. Catal. 185 (1999) 33.
[34] D.H. Olson, W.O. Haag, ACS Symp. Ser. 248 (1984) 275.
[35] S. Melson, F. Schüth, J. Catal. 170 (1997) 46.
[36] E. Klemm, H. Scheidat, G. Eming, Chem. Eng. Sci. 52 (1997) 2757.
[37] E. Klemm, J. Wang, G. Emig, Chem. Eng. Sci. 52 (1997) 3173.
[38] N. Arsenova-Härtel, H. Bludau, R. Schumacher, W.O. Haag, H.G. Karge, E. Brunner, U. Wild, J. Catal. 191 (2000) 326.
[39] M.A.V. Ribeiro da Silva, M.A.R. Matos, L.M.P.F. Amaral, J. Chem. Thermodyn. 27 (1995) 565.
[40] S.J. Jong, A.R. Pradhan, J.F. Wu, T.C. Tsai, S.B. Liu, J. Catal. 174 (1998) 210.
[41] G. Engelhardt, D. Michel, High-Resolution Solid-State NMR of Silicates and Zeolites, Wiley, New York, 1987 (Chapter V).
[42] L. Baltusis, J.S. Frye, G.E. Maciel, J. Am. Chem. Soc. 108 (1986) 7119.
[43] J.H. Lunsford, Top. Catal. 4 (1997) 91.
[44] E.F. Rakiewicz, A.W. Peters, R.F. Wormsbecher, K.J. Sutovich, K. Muller, J. Phys. Chem. B 102 (1998) 2890.
[45] K.J. Sutovich, A.W. Peters, E.F. Rakiewicz, R.F. Wormsbecher, S.M. Mattingly, K. Muller, J. Catal. 183 (1999) 155.
[46] C.E. Webster, R.S. Drago, M.C. Zerner, J. Am. Chem. Soc. 120 (1998) 5509.
[47] I.V. Mishin, H.K. Beyer, H.G. Karge, Appl. Catal. A 180 (1999) 207.
[48] J.C. Védrine, A. Auroux, V. Bolis, P. Dejaifve, C. Nacache, P. Wierzchowski, E.G. Derouane, J.B. Nagy, J.P. Gilson, J.H.C. van Hooff, J.P. van de Berg, J. Wolthuizen, J. Catal. 59 (1979) 248.
[49] A. Auroux, V. Bolis, P. Wierzchowski, P.C. Gravelle, J.C. Védrine, J. Chem. Soc., Faraday Trans. 175 (1979) 2544.
[50] G.L. Haller, Catal. Rev.-Sci. Eng. 23 (1981) 477.
[51] J.A. Lercher, C. Gründling, G. Eder-Mirth, Catal. Today 27 (1996) 353.
[52] W.H. Chen, J.S. Jong, A. Pradhan, T.Y. Lee, I. Wang, T.C. Tsai, S.B. Liu, J. Chin. Chem. Soc. 43 (1996) 305.
[53] J. Fraissard, T. Ito, Zeolites 8 (1988) 350.
[54] T. Ito, J.L. Bonardet, J.P. Fraissard, J.B. Nagy, C. Andre, Z. Gabelica, E.G. Derouane, Appl. Catal. 43 (1988) L5.
[55] N.R.E.N. Impens, P. van der Voort, E.F. Vansant, Microp. Mesop. Mater. 28 (1999) 217.
[56] T.C. Tsai, I. Wang, Appl. Catal. 77 (1991) 209.
[57] P.J. Grobet, H. Geerts, M. Tielen, J.A. Martens, P.A. Jacobs, Stud. Surf. Sci. Catal. 46 (1989) 721.
[58] E. Brunner, H. Ernst, D. Freude, T. Fröhlich, M. Hunger, H. Pfeifer, Stud. Surf. Sci. Catal. 49A (1989) 623.
[59] P.P. Man, J. Klinowski, Chem. Phys. Lett. 147 (1988) 581.
[60] J.H. Kim, T. Kunieda, M. Niwa, J. Catal. 173 (1998) 433.
[61] Y. Sendoda, Y. Ono, Zeolites 8 (1988) 101.
[62] M. Niwa, M. Kato, T. Hattori, Y. Murakami, J. Phys. Chem. 90 (1986) 6233.
[63] T.C. Tsai, S.B. Liu, I. Wang, Appl. Catal. A 181 (1999) 355.
[64] M.A. Uguina, J.L. Sotelo, D.P. Serrano, Ind. Eng. Chem. Res. 32 (1993) 49.
[65] N.Y. Chen, T.F. Degnan Jr., C.M. Smith, Molecular Transport and Reaction in Zeolites: Design and Application of Shape Selective Catalysts, VCH Publishers, New York, 1994.